The inter-scale behaviour of two natural scaly clays

Géotechnique Letters

The inter-scale behaviour of two natural scaly clays

--Manuscript Draft--

Manuscript Number:	
Full Title:	The inter-scale behaviour of two natural scaly clays
Article Type:	Paper
Corresponding Author:	Vincenzo Nardelli, M.D. City University of Hong Kong Hong Kong, HONG KONG
Corresponding Author Secondary Information:	
Corresponding Author's Institution:	City University of Hong Kong
Corresponding Author's Secondary Institution:	
First Author:	Vincenzo Nardelli, M.D.
First Author Secondary Information:	
Order of Authors:	Vincenzo Nardelli, M.D.
	Matthew Richard Coop, PhD
	Claudia Vitone, PhD
	Sihua Chen, BSc
Order of Authors Secondary Information:	
Abstract:	This paper describes the results of an experimental investigation of the inter-scale behaviour of two natural scaly clays. These have been tested by means of a custom-made inter-particle loading apparatus, which has enabled their mechanical response to be studied in both compression and shearing. The main features of the micromechanical behaviour of these clays have been compared, focusing on the influence of their composition, and the results compared with those obtained testing the same materials using other devices (triaxial and ring shear apparatus). The results have shown that, contrary to expectations, the surfaces of the scales are not residual shear surfaces and the inter-scale angle of shearing resistance is actually closer to critical state or post-peak angles measured in conventional tests.

The inter-scale behaviour of two natural scaly clays

V. Nardelli, M.R. Coop, C. Vitone and S. Chen

Word count: 2000

Abstract

This paper describes the results of an experimental investigation of the inter-scale behaviour of two natural scaly clays. These have been tested by means of a custom-made inter-particle loading apparatus, which has enabled their mechanical response to be studied in both compression and shearing. The main features of the micromechanical behaviour of these clays have been compared, focusing on the influence of their composition, and the results compared with those obtained testing the same materials using other devices (triaxial and ring shear apparatus). The results have shown that, contrary to expectations, the surfaces of the scales are not residual shear surfaces and the inter-scale angle of shearing resistance is actually closer to critical state or post-peak angles measured in conventional tests.

Keywords: scaly clays, inter-scale behaviour, strength, stiffness, friction

List of symbols:

A	clay activity
CF	clay fraction
MF	silt fraction
PS	Pisciolo clay
SCM	Santa Croce di Magliano clay
SF	sand fraction
w_l	liquid limit
ϕ	inter-scale friction angle
ϕ^*_{cs}	critical state friction angle for the reconstituted clay
ϕ'_{peak}	friction angle at peak
$\phi'_{post\text{-}peak}$	post-peak friction angle
ϕ'_r	residual friction angle
μ	inter-scale coefficient of friction

1. Introduction

Scaly clays are natural materials characterised by an intensely fissured mesostructure, which originate from different geological processes, such as tectonic deformations, bulk shearing, submarine gravity sliding, often more recently modified by erosion and weathering. Generally, these materials appear as flaky aggregates made up of small elements called scales (Fig. 1a and b), which are visible to the naked eye and have dimensions that range from the millimetres to centimetres. Clay scales usually have a flat shape and feature polished, shiny or waxy surfaces (Vannucchi et al., 2003).

Although these materials are made up of distinct elements, the scales, their macro-scale behaviour usually is interpreted by means of continuum mechanics, for example Cotecchia and Santaloia (2003) and Vitone and Cotecchia (2011), who interpreted the mechanical behaviour of intensely fissured clays within the framework of CSSM. Vitone et al. (2013) observed that pre-existing fissures play an important rôle in the strain localisation while shearing samples of scaly clay in a plane strain apparatus. Vitone and Cotecchia (2011) introduced a fissuring characterisation chart, in order to classify and evaluate the Fissuring Identity (F-ID) of the fissured clays with respect to those features that affect their mechanical behaviour, such as intensity (I) and orientation (F) of fissures.

Previous experimental work at the micro-scale level have focussed on the micromechanical behaviour of sands, especially after these started to be studied by means of discrete mechanics (Cundall and Strack, 1979). Most of these works have examined the strength of sand particles (e.g., Nakata et al., 1999), while others have investigated the contact behaviour (Horn and Deere, 1962; Skinner, 1969; Cavarretta et al., 2010; Senetakis et al., 2013). However, it should be emphasised that while this work on sands has tested individual particles the current work is “micro” only in the sense that small structural elements of the natural clays have been tested, not single particles.

The materials tested in the present work are the scaly clays from Santa Croce di Magliano (SCM) and Pisciolo (PS), which are two localities in the Southern Apennines of Italy. They both belong to the so-called *structurally complex formations* (Croce, 1971; Esu, 1977), which are typically characterised by a fissured mesostructure originating from very large displacements related to regional tectonics. SCM clay belongs to the Red Flysch formation (Oligocene-Miocene, Dazzaro and Rapisardi, 1996), while the PS clay sample tested has been

ascribed to the upper unit of the Paola Doce formation (late Oligocene-lower Miocene, Cotecchia et al., 2015).

2. Equipment, materials tested and procedures

2.1 Inter-particle loading apparatus

The micromechanical experiments were carried out by means of the inter-particle loading apparatus (Fig. 2), which is custom built device originally designed to investigate the contact behaviour of sands (Senetakis and Coop, 2014). This is capable of applying different combinations of either forces or displacements at the contacts of a pair of soil particles in three directions. The apparatus was modified in order to increase the number of testing modes, minimise its compliance and improve the accuracy of the displacement measurements (Nardelli and Coop, 2014).

The apparatus consists of a stiff stainless steel loading frame, a stainless steel sled and three loading arms (a and b in Fig. 2). One loading arm is oriented along the vertical direction while the other two are in orthogonal horizontal directions. Each loading arm was comprised of a micro linear actuator (Fig. 2c) and a load cell, connected the sled and particle mounts by means of stiff mechanical parts. The sled is placed on a polished piece of stainless steel by means of a bearing system made up of three chrome steel balls and can be moved along the horizontal plane by means of the linear actuators. The upper particle is held by a holder placed at the end of the vertical loading arm, which applies the vertical load at the contact with the lower particle during shearing (Fig. 2d). The forces are measured by means of high-resolution load cells (Fig. 2e) having a capacity of 100N.

In the modified version of the apparatus, the displacements are measured using three non-contact eddy current displacement sensors (Fig. 2f), which have a measuring range of 3mm and a resolution of 10^{-5}mm. The whole apparatus is located inside a Perspex chamber and the humidity conditions of this are controlled using a humidity controller that is able to regulate the relative humidity within a range between 15% and 85%. Two digital micro-cameras (Fig. 2g) are installed inside the Perspex chamber. These help to find the right location and orientation of the contact between the two loaded surfaces and to record images during each test.

2.2 Materials tested

The particular SCM clay sample used for these tests was characterised by a very high fissuring intensity (I6) and with fissures orientated at 45° to the horizontal (F1-45) according to the F-ID classification chart of Vitone and Cotecchia (2011). Also, it featured a very high clay fraction (CF=91%), medium activity (A=0.70) and high liquid limit (w_l=97%). As reported by Vitone and Cotecchia (2011), the SCM clay was more generally characterised by a similar clay fraction (CF=91%), but lower activity (A=0.57) and liquid limit (w_l=81%) in their previous investigations. The SCM clay scales tested had an average thickness of 0.94mm and length of 3.24mm.

The particular Pisciolo clay sample tested featured a lower fissuring intensity (I6/I5) and a set of fissures randomly orientated (F3). Its clay fraction was lower (CF=45%), its content of silt and sand much higher (MF=30%, SF=21%) and liquid limit lower (w_l=60%) compared with the SCM clay sample, while the activity (A=0.75) was also medium. As outlined in Cotecchia et al. (2015), the upper unit of Paola Doce formation, where PS clay belongs to, more generally exhibits clay fractions within the range 19-55%, sand fractions that are significant (SF=16-26%) and activities from medium to high (A=0.5-1). The PS clay scales tested had an average thickness of 1.17mm and length of 3.18mm.

2.3 Testing procedures

The clays were tested using both the inter-particle loading apparatus and the Bromhead ring shear apparatus. For the inter-scale tests, these were carried out applying either forces or displacements at the contact of two scales of clay mounted on stiff brass holders using a thin layer of super glue. The structure of each clay scale was preserved in order to test them in conditions that were as close as possible to those in situ. The samples were prepared taking care of the scale shape, selecting the pieces of soil having a defined clay scale structure which was characterised by a flat shape so that two parallel faces could be tested, in order to minimise the components of force out of plane. Most of the tests were performed on scales taken directly from the undisturbed clay specimen at their natural water content, but for some others a small amount of distilled water was sprayed on the top of their surface before placing them inside the apparatus. This was done to check whether any pore water suction at the scale contact might affect the data, and was done immediately before loading to avoid softening of the surfaces.

The ring shear tests were carried out using two different procedures: a *standard* one, in which the material was remoulded at a water content around $1.5w_l$, and an *alternative* one where portions of intact material were taken directly from the clay sample and placed inside the ring of the apparatus, orientating the existing fissures along the shearing direction. All the tests were performed shearing the samples at the minimum velocity allowed by the apparatus (0.019mm/min), after consolidation to maximum vertical effective stresses between 107kPa and 300kPa.

3. Results

3.1 Compression behaviour at the scale contacts

Of primary interest is the inter-scale shearing behaviour, but the initial normal loading data are presented for completeness. Figure 3 shows the results of the initial vertical compression stages for both the SCM and PS clays. In each test, the clay scales were compressed along the direction normal to the contact between the scales, using displacement rates between 0.2 and 0.8mm/h, while the material was unconfined laterally. The behaviour typically observed is characterised by an elasto-plastic response that becomes stiffer with the increase of the normal displacement. The data are quite scattered, and it is likely that the response is sensitive to the scale geometry and surface morphology. The stiffness of most of the curves at higher loads tends to a similar value, although some scales pairs exhibit softer behaviour. For displacements larger than 0.02mm, PS clay seems to be less compressible than the SCM clay, probably because of his lower clay fraction and lower plasticity index.

Figure 4 shows the results of a test where two SCM clay scales were loaded up to 3N, then unloaded and reloaded reaching 3N again. The test shows that the unloading-reloading behaviour is completely reversible and the material reaches the maximum load after a hysteresis loop. It can also be seen that no suction was measured between the scales on unloading, as the vertical load does not become negative, which was observed for all the tests performed on both clays.

3.2 Shearing behaviour of the scale contacts

Twenty-two shear tests were carried out on the SCM scaly clay and fourteen on the PS clay, confined under normal loads between 1N (the limit for accurate data in this apparatus) and 10N and sheared applying displacement rates of between 0.02 and 0.08mm/h. Figures 5 and 6 show the tangential force-displacement curves for the SCM and PS clays, respectively. In

general the tests were terminated as soon as a constant tangential force was reached, but some tests were continued to larger displacements to check whether the measured force would degrade. Both graphs show that the two clays exhibit a similar behaviour in shearing, where the response becomes less stiff with the increase of the displacement until a steady state is reached. Also, the clay behaviour seems to be dependent on the applied vertical load during shearing. This dependence can be also observed in the tangential stiffnesses (Figs. 7 and 8), which decrease with the increase of the displacement until it reaches values around zero, corresponding to the steady state. Some scatter can also be observed for tests carried out under the same confining loads, especially for the SCM clay.

Figure 9 illustrates the results of a cyclic shear test on a pair of SCM clay scales vertically confined under 3N. The slope of the unloading and reloading curves seems not to be affected by the increase of the number of loops and a degradation of the stiffness is not evident. Also, a slight decrease of friction coefficient can be observed between the steady state reached at small displacements (0.02-0.04mm) and that after large displacements (over 0.1mm).

Figure 10 shows the results obtained for both SCM and PS clays plotted normalising the tangential load by means of the vertical load during each test. The continuous lines represent the tests carried out under low vertical loads (1-3N) while the dashed lines are for those under high forces (5-10N). This shows that slightly higher friction coefficients are generally reached for tests under low confining forces and that the curves obtained from these tests have a higher slope (i.e., normalised tangential stiffness) compared with those tests performed under higher confining forces. Also, the SCM clay response appears stiffer than that of PS clay.

The failure envelopes for both SCM and PS clays are shown in Figure 11. Small markers are used for those data obtained from tests performed spraying the clay scales using distilled water, while the large markers are for the remaining tests. The data for the two soils are remarkably similar, and both can be well represented with linear failure envelopes, despite the observation on Figure 10 that the mobilised stress ratios at low vertical forces are slightly higher. The PS clay exhibits values of friction coefficient between the scales that are slightly larger than those for the SCM clay, which may be caused by the higher silt and sand fractions of this material. The presence or absence of the sprayed water also makes no clear difference, again indicating that suctions do not play any significant rôle. The absence of an intercept on the failure envelope is a further confirmation that there are no significant inter-scale suctions.

Another important feature of the data is that they are reasonably consistent. Considering that the horizontal orientation of the scales was random, this is an indication there are unlikely to be different mobilised angles of shearing resistance in different directions.

3.3 Comparisons with macro-scale test results

Figure 12 illustrates the results of the tests carried out on both SCM and PS clays by means of the ring shear apparatus. The average residual friction angles obtained by means of the standard procedure, which involves the remoulding of the natural material, are slightly larger than those obtained from the alternative procedure. The values obtained are consistent with the correlations proposed by Lupini et al. (1981), which relate the residual friction angle with the clay fraction and the plasticity index.

Table 1 shows a summary of the friction angles measured on SCM and PS clays from the literature. Only the ring shear data obtained from the standard process are presented. It shows that the friction angles obtained from the inter-scale tests are much higher than the residual ones, and they are close to the post-peak values determined through the triaxial tests, generally determined for the samples experiencing failure along a shear band that localised along the pre-existing fissures. They are also quite similar to the critical state values determined from tests on reconstituted samples and also the "peak" values from the ring shear tests, although the latter would not be reliable peak strengths because of progressive failure due to varying strains across the sample radius. This means that the clay platelets on the surface of the contacting scales are not flat and aligned. Despite their appearance and genesis a strength that is much higher than the residual is mobilised on the clay scales.

4. Conclusions

This work has focussed on the inter-scale behaviour of two natural scaly clays from Italy, which was studied by means of a custom-made inter-particle loading apparatus. The results showed that despite the lower clay content and lower plasticity of the Pisciolo clay the mobilised inter-scale angle of shearing resistance is very similar to that of the clay from Santa Croce di Magliano. A comparison between the micro-scale test results and those obtained from tests on macro-scale samples using the ring shear and triaxial apparatuses showed that the strength measured on the surface between two clay scales is far from the residual strength, and more similar to post-peak or critical state strengths, so it is unlikely that there is alignment of the clay platelets on the surfaces of the scales.

ACKNOWLEDGMENTS

The Authors would like to thank Professor Federica Cotecchia for providing the scaly clays tested in this research project. They are also grateful to Dr Béatrice Baudet for the use of the ring shear apparatus at the University of Hong Kong. The technicians of City University of Hong Kong, Mr Y.H. Tsang and C.K. Lai and Mr E. Miccoli of Technical University of Bari are also acknowledged for their help, along with Mr V. Roca and F. Carone that performed the ring shear tests at the Technical University of Bari. Also, the Authors would like to thank Dr G. Pedone for sampling the Pisciolo clay. This work was fully supported by a grant from the Research Grants Council of the Hong Kong Special Administrative Region, China (Project No. CityU 112712).

REFERENCES

Cavarretta, I., Coop, M.R. & O'Sullivan, C. (2010). The influence of particle characteristics on the behaviour of coarse grained soils. *Géotechnique*, **60** (6), 413-423.

Cotecchia, F. & Santaloia, F. (2003). Compression behaviour of structurally complex marine clays. *Proc. Nakase Memorial Symposium on "Soft Ground Engineering in Coastal Areas"*, Yokosuka, Japan, 63-72.

Cotecchia F, Vitone, C., Santaloia, F., Pedone, G. & Bottiglieri, O. (2015). Slope instability processes in intensely fissured clays: case histories in the Southern Apennines. *Landslides*, **12** (5), 877-893.

Croce, A. (1971). *Opening address of the Int. Symp. "The Geotechnics of structurally complex formations"*. Capri, **2**, 148-151.

Cundall, P.A. & Strack, O.D.L. (1979). A discrete numerical model for granular assemblies. *Géotechnique*, **29** (1): 47–65.

Dazzaro, L. & Rapisardi, L. (1996). Schema geologico del margine appenninico tra il F.Fortore e il F.Ofanto. *Memorie della Società Geologica Italiana*, **51**, 143-147.

Horn, H.M. & Deere, M.S. (1962). Frictional characteristics of minerals. *Géotechnique*, **12** (4), 319-335.

Esu, F. (1977). Behaviour of slopes in structurally complex formations. *The Geotechnics of Structurally Complex Formations, Proc. Intern. Symp*., Capri, **2**, 292-304.

Lupini, J.F., Skinner, A.E. and Vaughan, P.R. (1981). The drained residual strength of cohesive soils. *Géotechnique*, **31** (2), 181-213.

Nakata, Y., Hyde, A.F.L., Hyodo, M. & Murata, H. (1999). A probabilistic approach to sand crushing in the triaxial test. *Géotechnique*, **49** (5), 567-583.

Nardelli, V. & Coop, M.R. (2014). An experimental investigation of the micromechanical behaviour of cemented sand particles. *Proceedings of the TC105 ISSMGE International Symposium on Geomechanics from Micro to Macro*, Cambridge, UK, 1-3 September 2014, **2**, 1013-1018.

Senetakis, K. & Coop, M.R. (2014). The development of a new micro-mechanical inter-particle loading apparatus. *Geotechnical Testing Journal*, **37** (6), 1028-1039.

Senetakis, K., Coop, M.R. & Todisco. M. C. (2013). Tangential load-deflection behaviour at the contacts of soil particles. *Géotechnique Letters* **3** (2), 59-66.

Skinner, A.E. (1969). A note on the influence of interparticle friction on shearing strength of a random assembly of spherical particles. Technical note. *Géotechnique*, **19** (1), 150-157.

Vannucchi, P., Maltman, A., Bettelli, G. & Clennell, M. (2003). On the nature of scaly clay fabric and scaly clay. *Journal of Structural Geology*, **25** (5), 673-688.

Vitone, C. & Cotecchia, F. (2011). The influence of intense fissuring on the mechanical behaviour of clays. *Géotechnique*, **61** (12), 1003-1018.

Vitone, C., Viggiani, G., Cotecchia, F. & Hall, S.A. (2013). Localized deformation in intensely fissured clays studied by 2D digital image correlation. *Acta Geotechnica*, **8** (3), 247-263.

(a) (b)

Figure 1. a) Mesostructure of PS clay; b) pair of scales of SCM clay before testing.

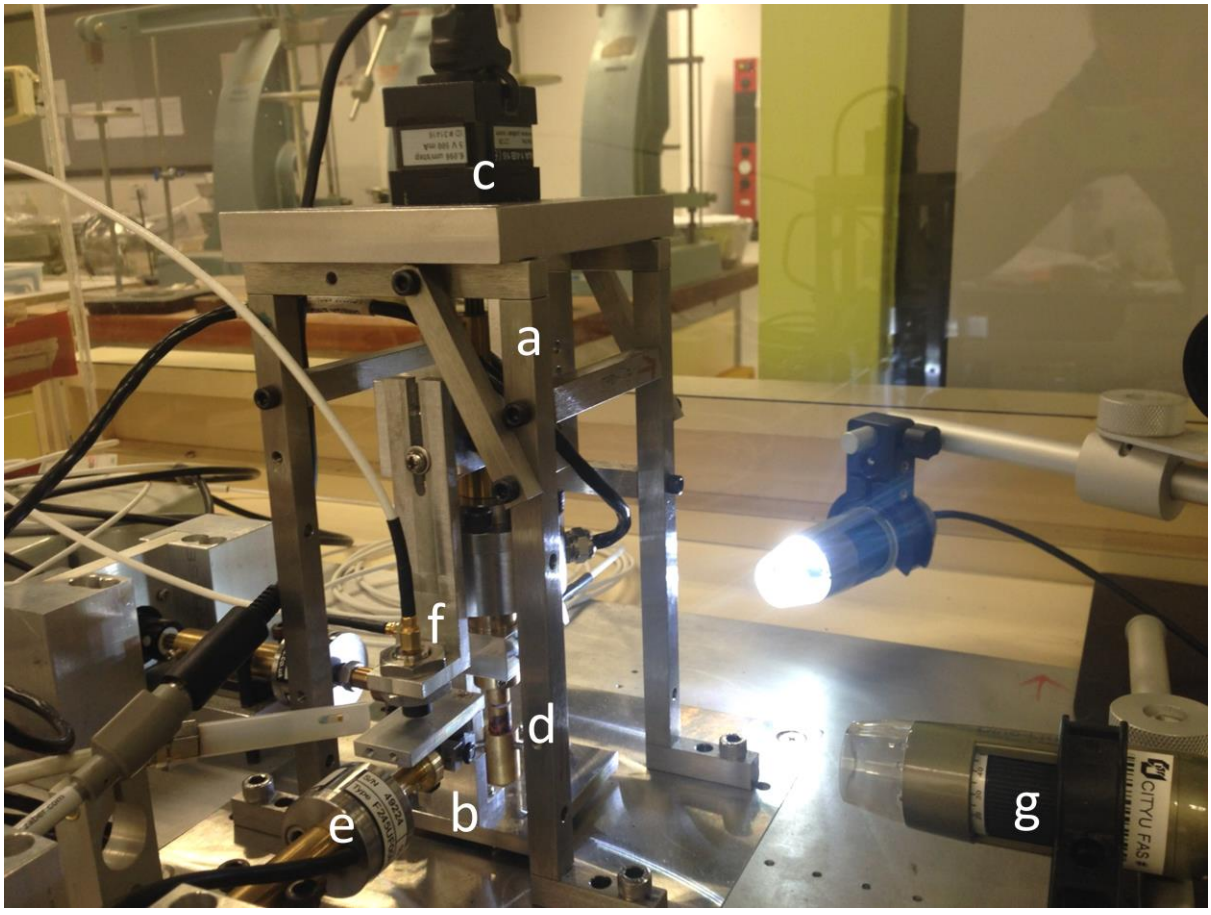

Figure 2. Inter-particle loading apparatus: a) loading frame; b) stainless steel sled; c) linear actuator; d) clay scales during a test; e) load cell; f) eddy-current displacement sensor; g) digital micro-camera.

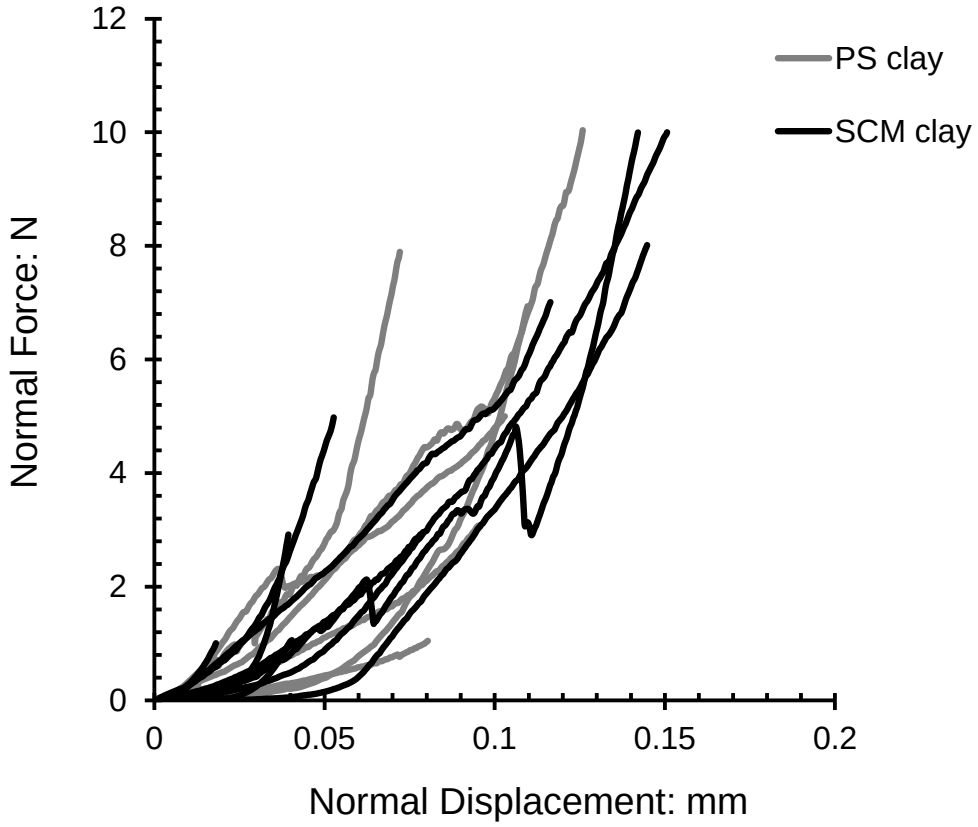

Figure 3. Comparison between the compression curves for both SCM and PS clays.

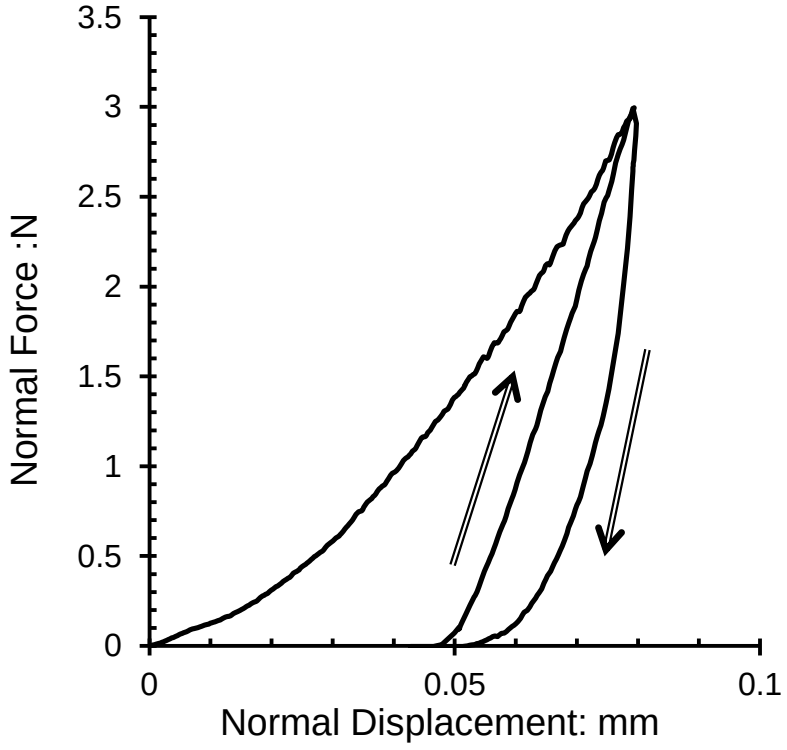

Figure 4. Loading-unloading-reloading behaviour of SCM clay in compression.

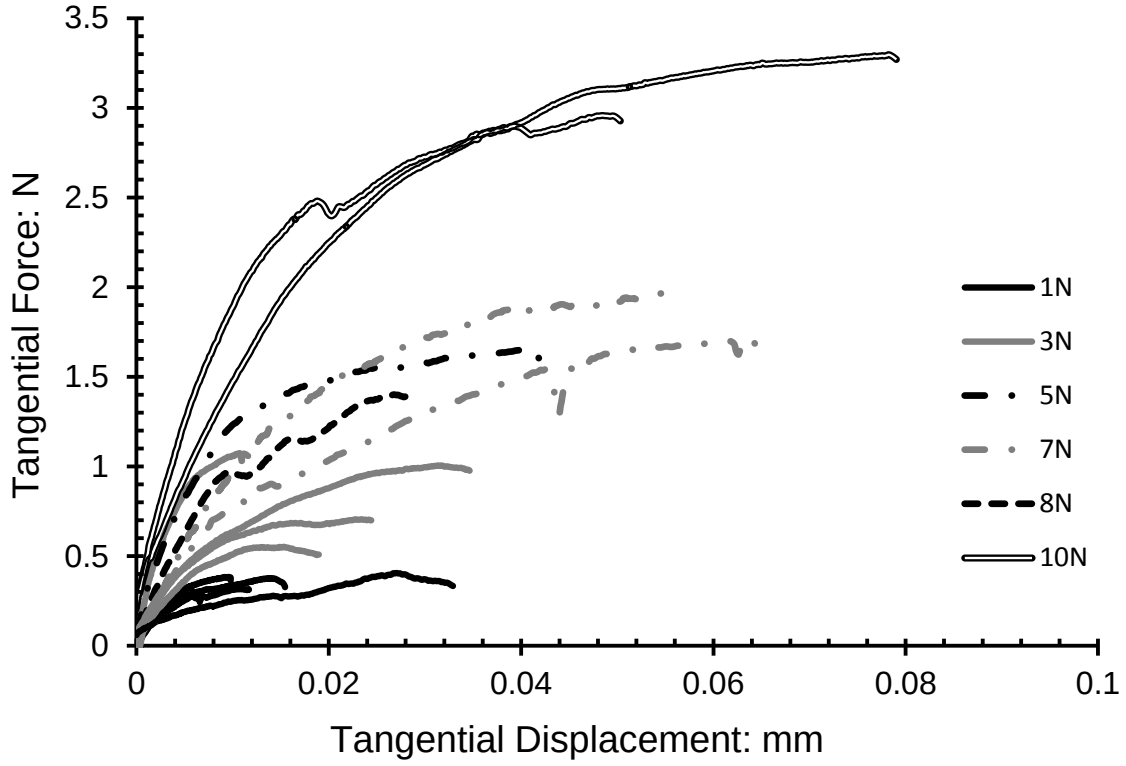

Figure 5. Tangential force-displacement curves for SCM clay scales.

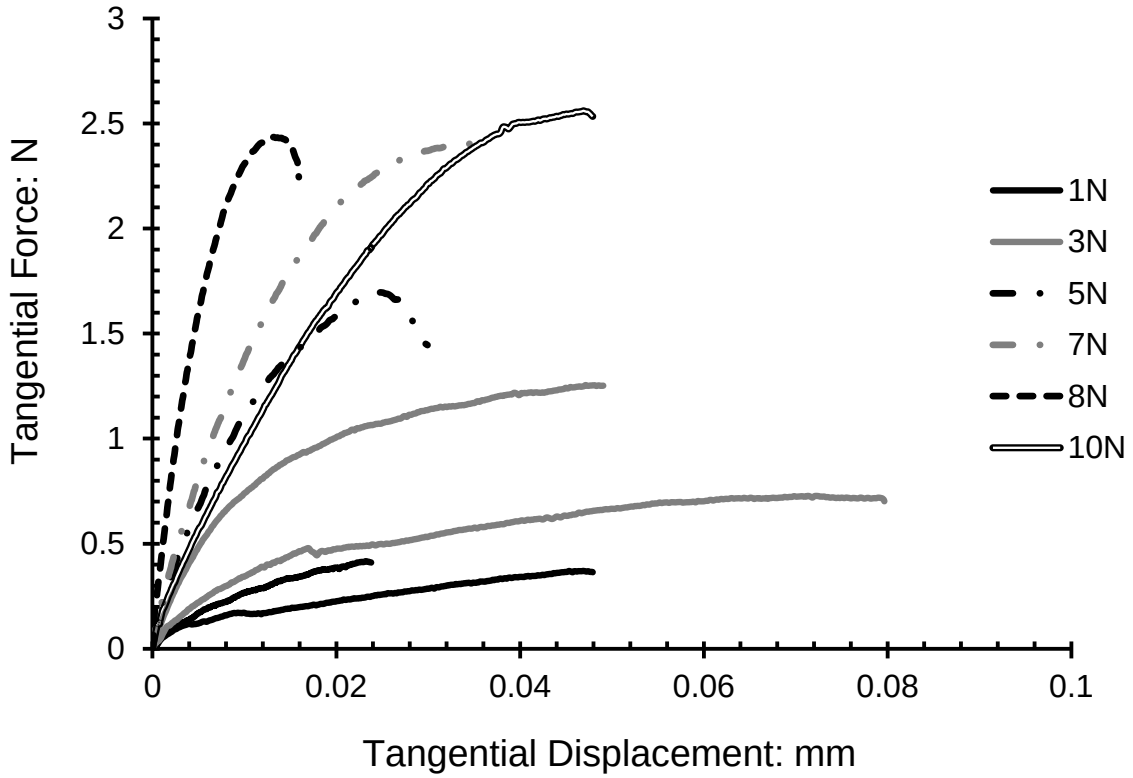

Figure 6. Tangential force-displacement curves for PS clay scales.

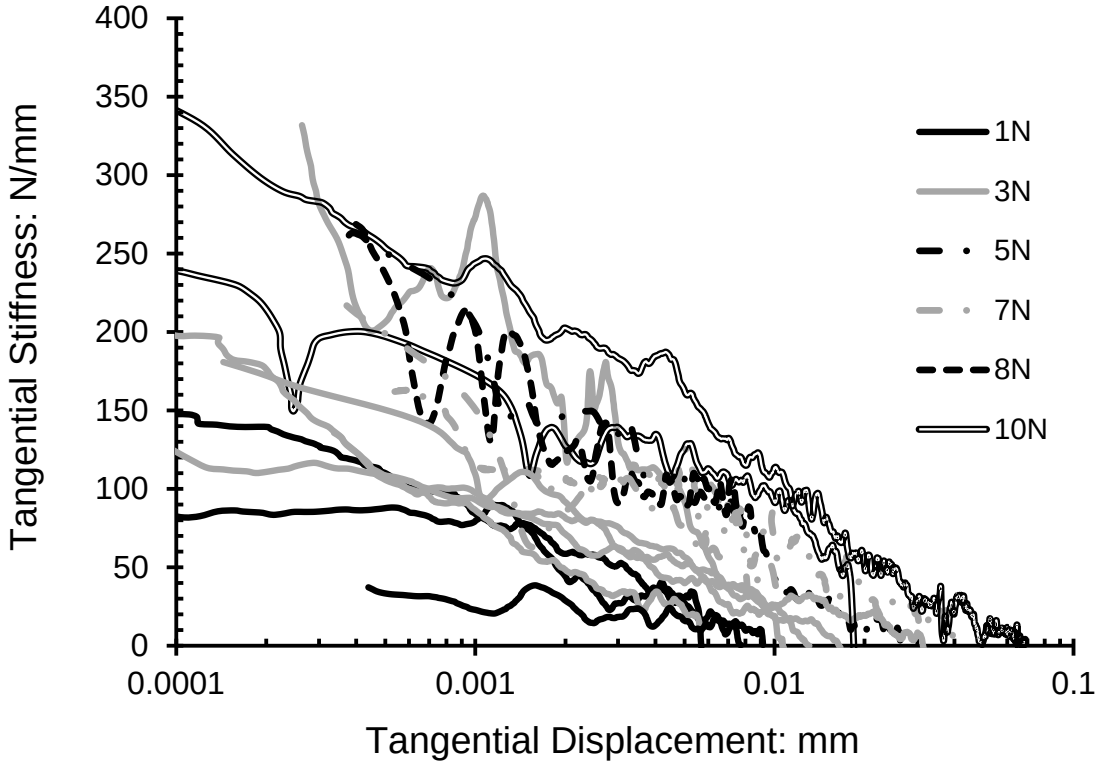

Figure 7. Tangential stiffness-displacement curves for SCM clay scales.

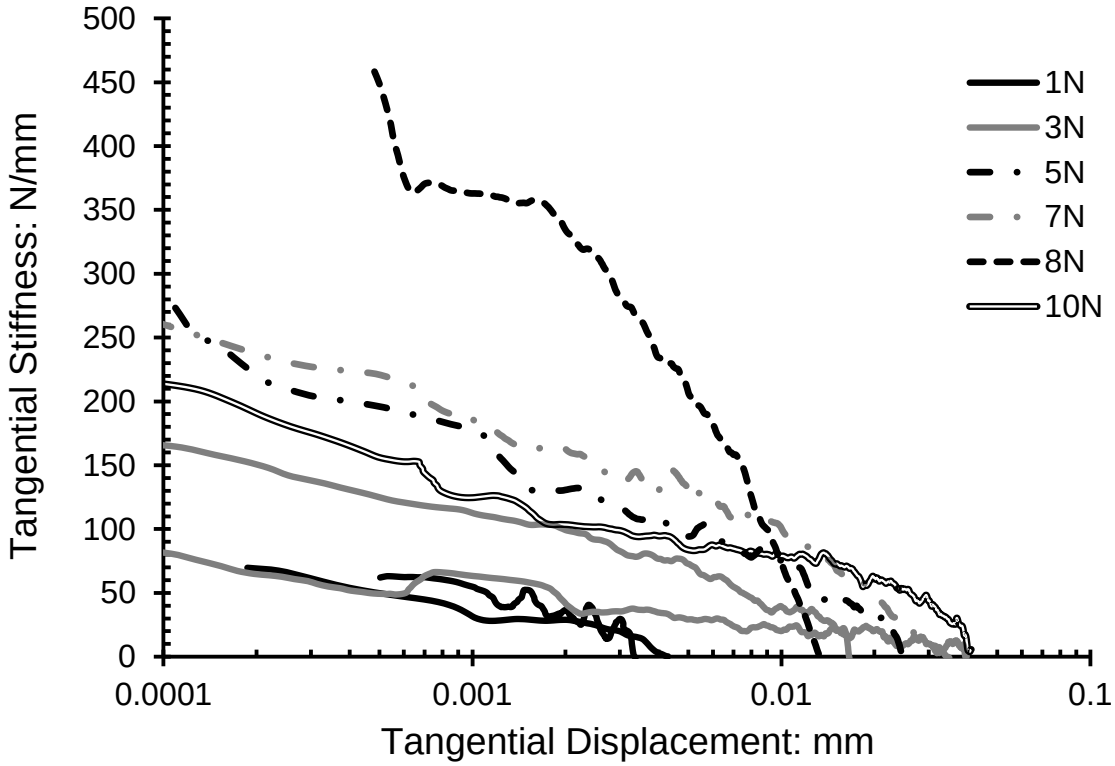

Figure 8. Tangential stiffness-displacement curves for PS clay scales.

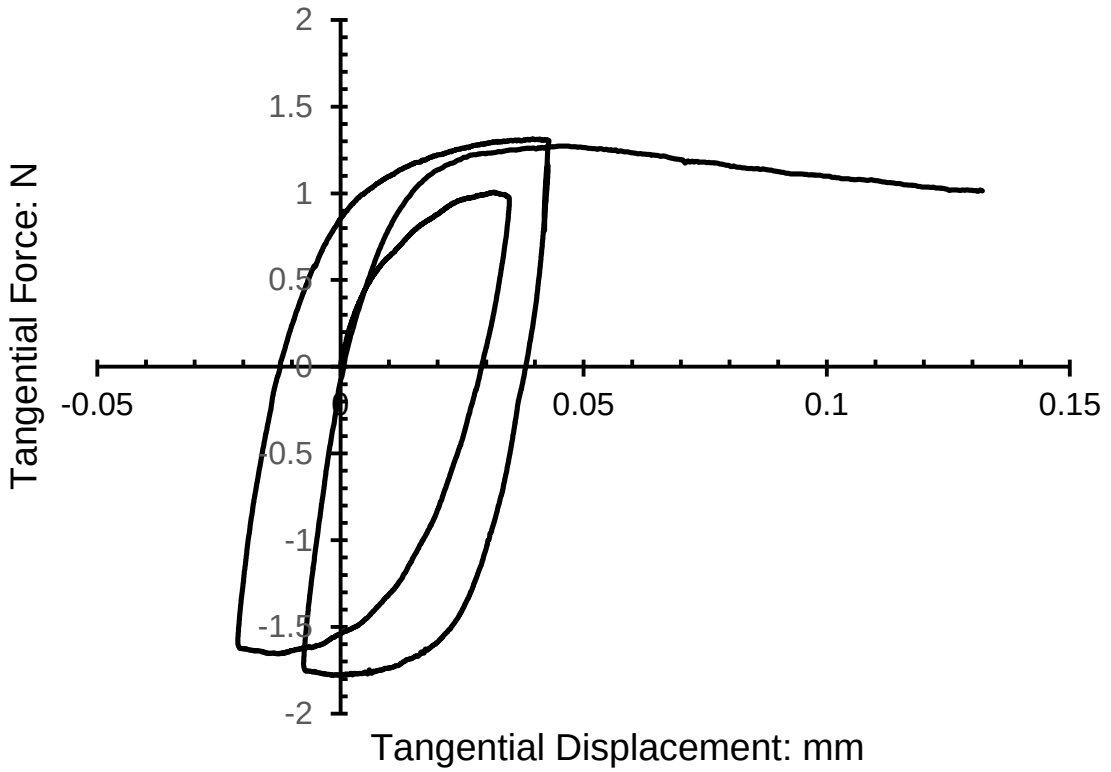

Figure 9. Cyclic tangential force-displacement curves for a pair of SCM clay scales under a normal load of 3N.

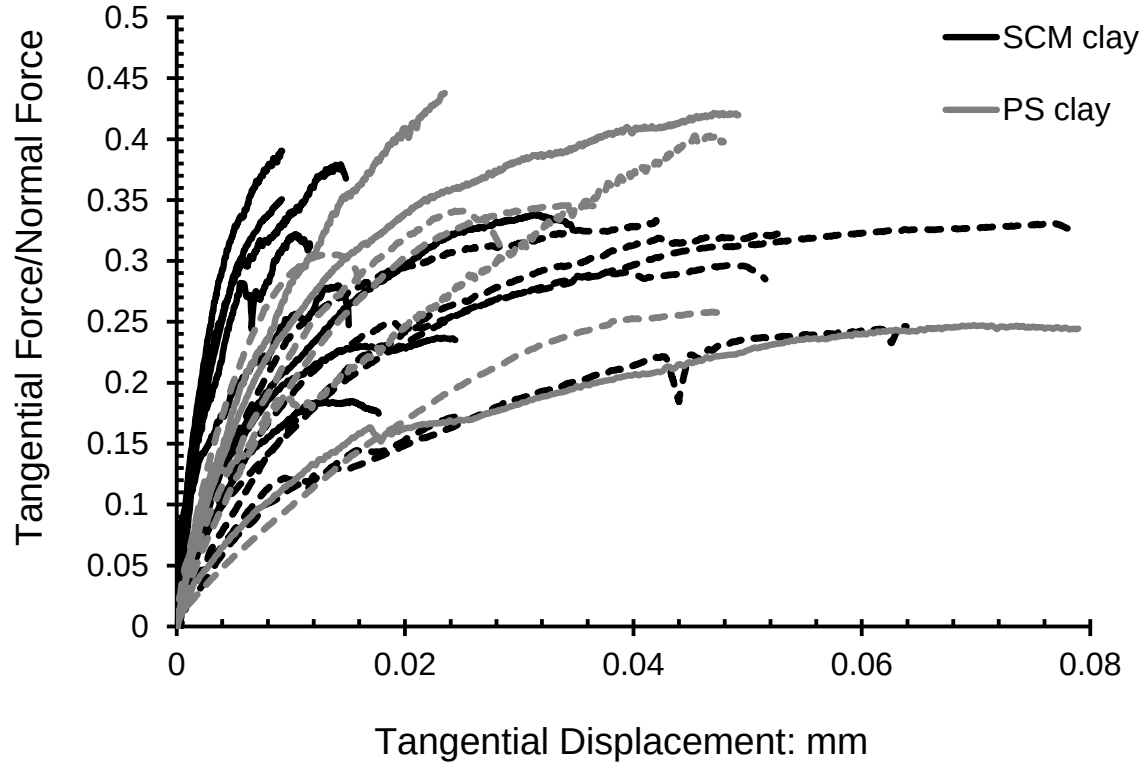

Figure 10. Comparison between the normalised tangential load-displacement curves of both SCM and PS clays: continuous lines for normal loads 1-3N, dashed lines for 5-10N.

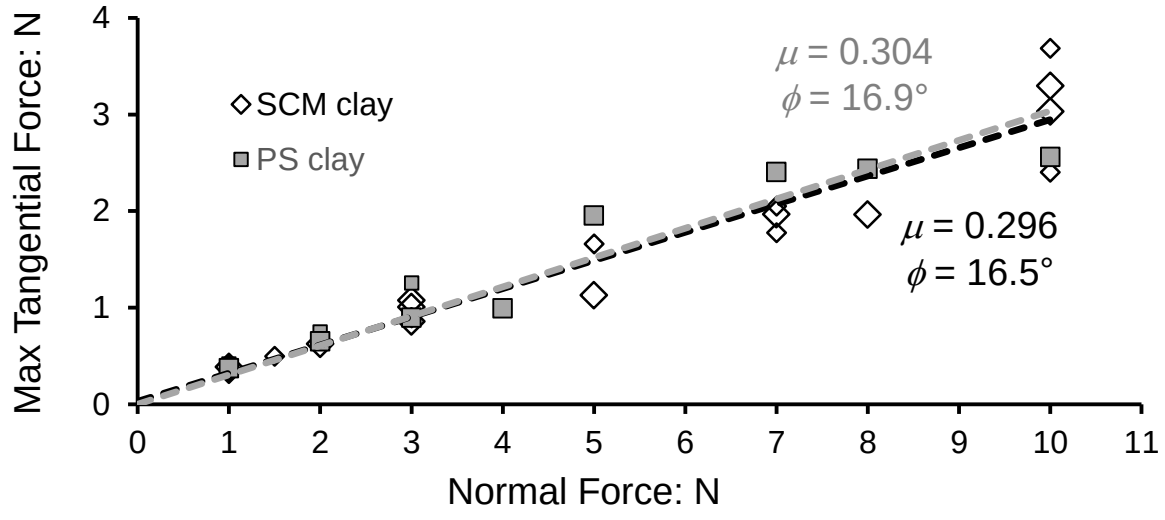

Figure 11. Failure envelopes for both SCM and PS scaly clays (small markers – water sprayed onto scale surfaces).

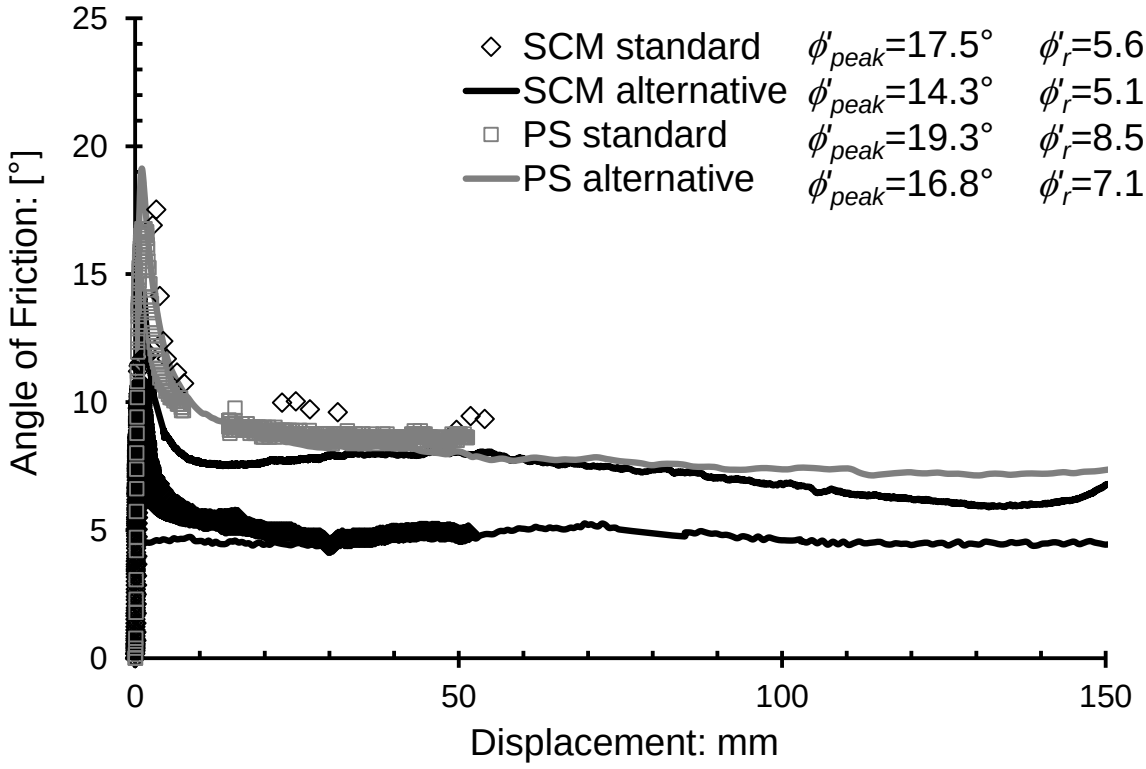

Figure 12. Ring shear test results for both SCM and PS scaly clays.

Table 1. Summary of the friction angles found here and in the literature for SCM and PS scaly clays.

Soil type	Testing device	Friction angle
SCM clay	Triaxial apparatus†	ϕ'_{peak}=25°, $\phi'_{post\text{-}peak}$=12-20° ϕ^*_{cs}=18°
	Ring shear apparatus	ϕ'_{peak}=17.5°, ϕ'_{r}=5.6°
	Inter-particle loading apparatus	ϕ =16.5°
PS clay	Triaxial apparatus§	ϕ'_{peak}=21-25°, $\phi'_{post\text{-}peak}$=13-20° ϕ^*_{cs}=18°
	Ring shear apparatus	ϕ'_{peak}=19.3°, ϕ'_{r}=8.5°
	Inter-particle loading apparatus	ϕ =16.9°

†: data from Vitone and Cotecchia (2011)

§: data from Cotecchia et al. (2014)

Figure 1a

Click here to download Figure Figure 1a.tif

Figure 1b

Click here to download Figure Figure 1b.tif

Figure 2

Click here to download Figure Figure 2.tif

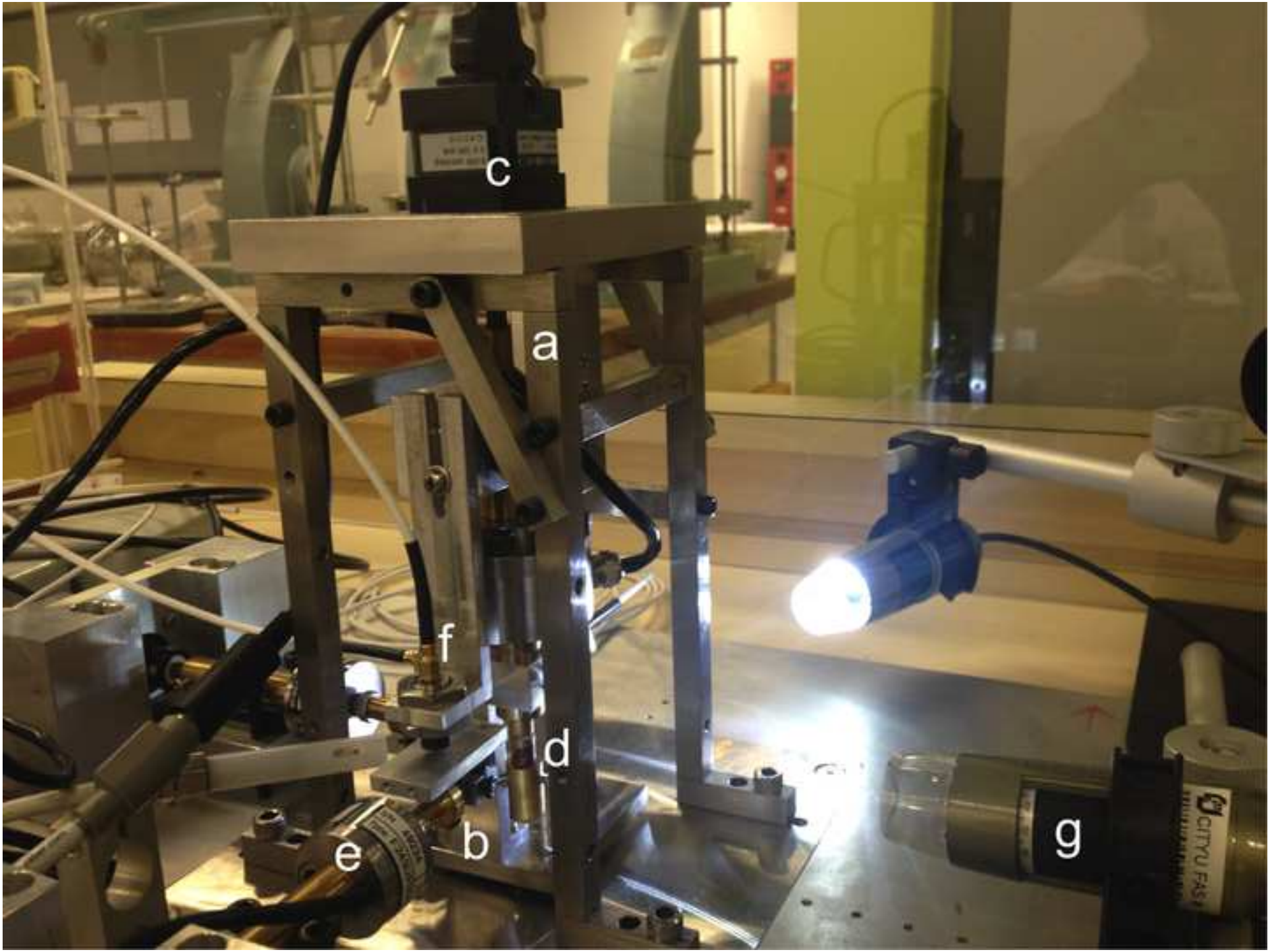

Figure 3

Click here to download Figure Figure 3.xlsx

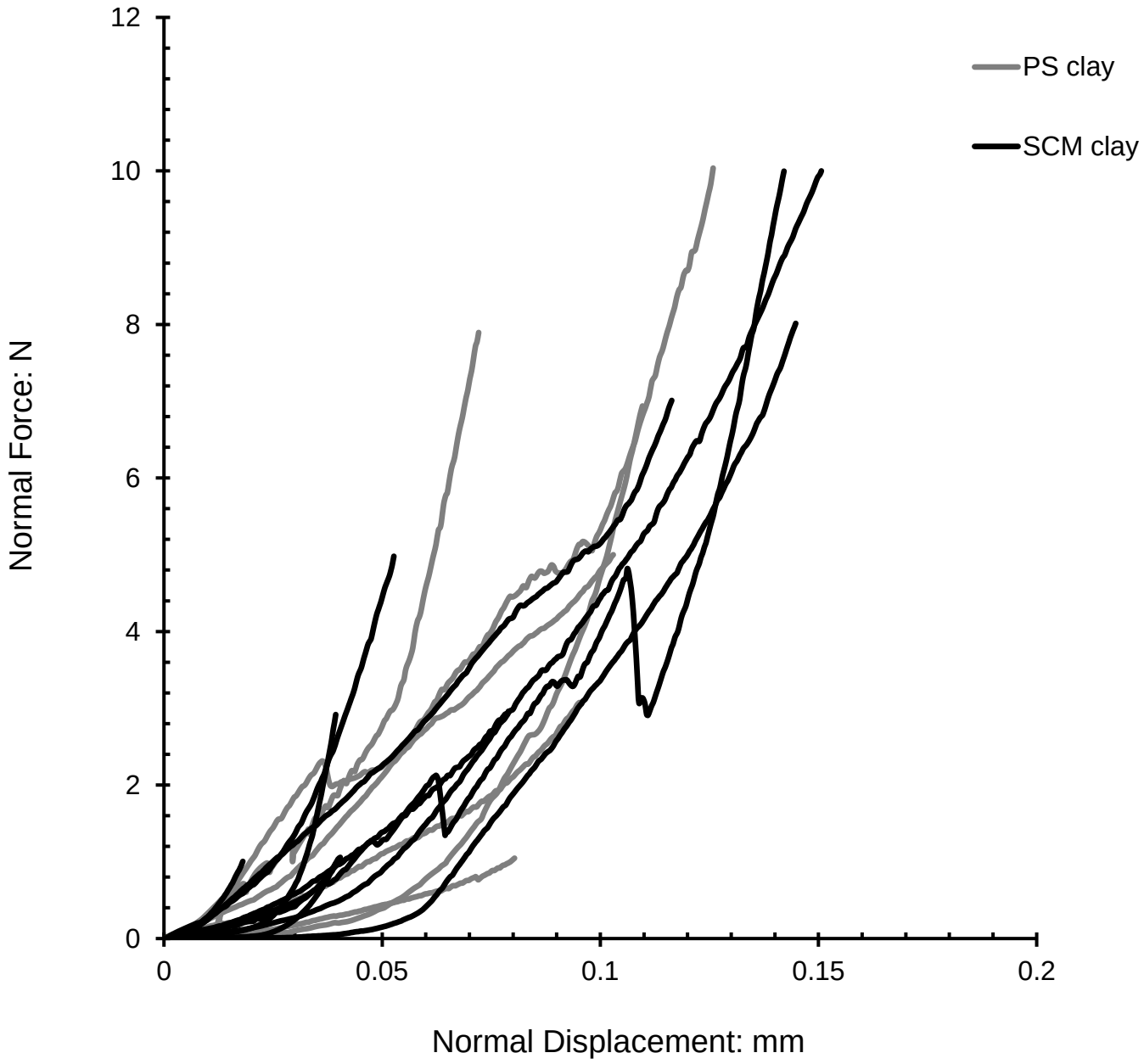

Figure 4

Click here to download Figure Figure 4.xlsx

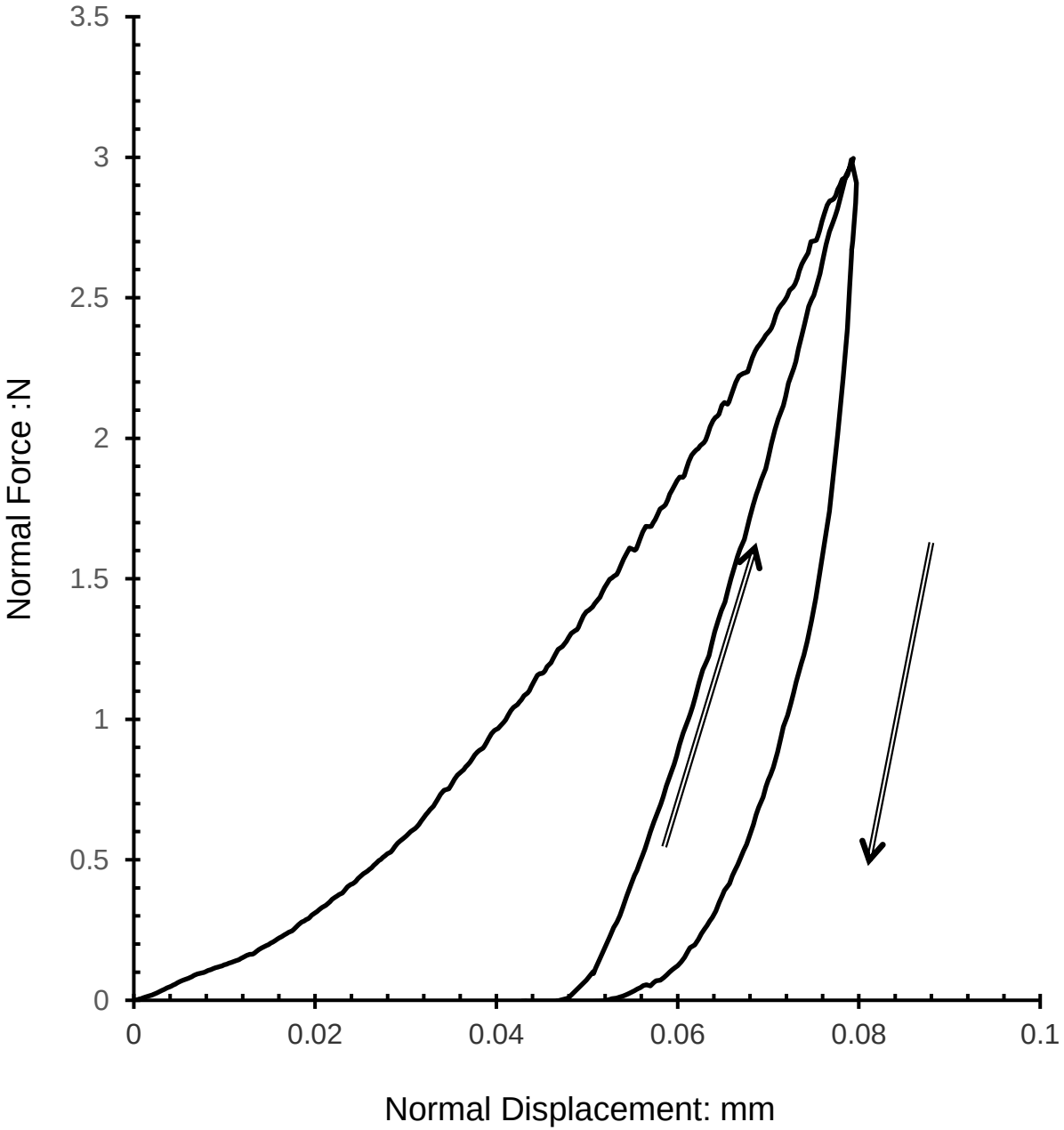

Figure 5

Click here to download Figure Figure 5.xlsx

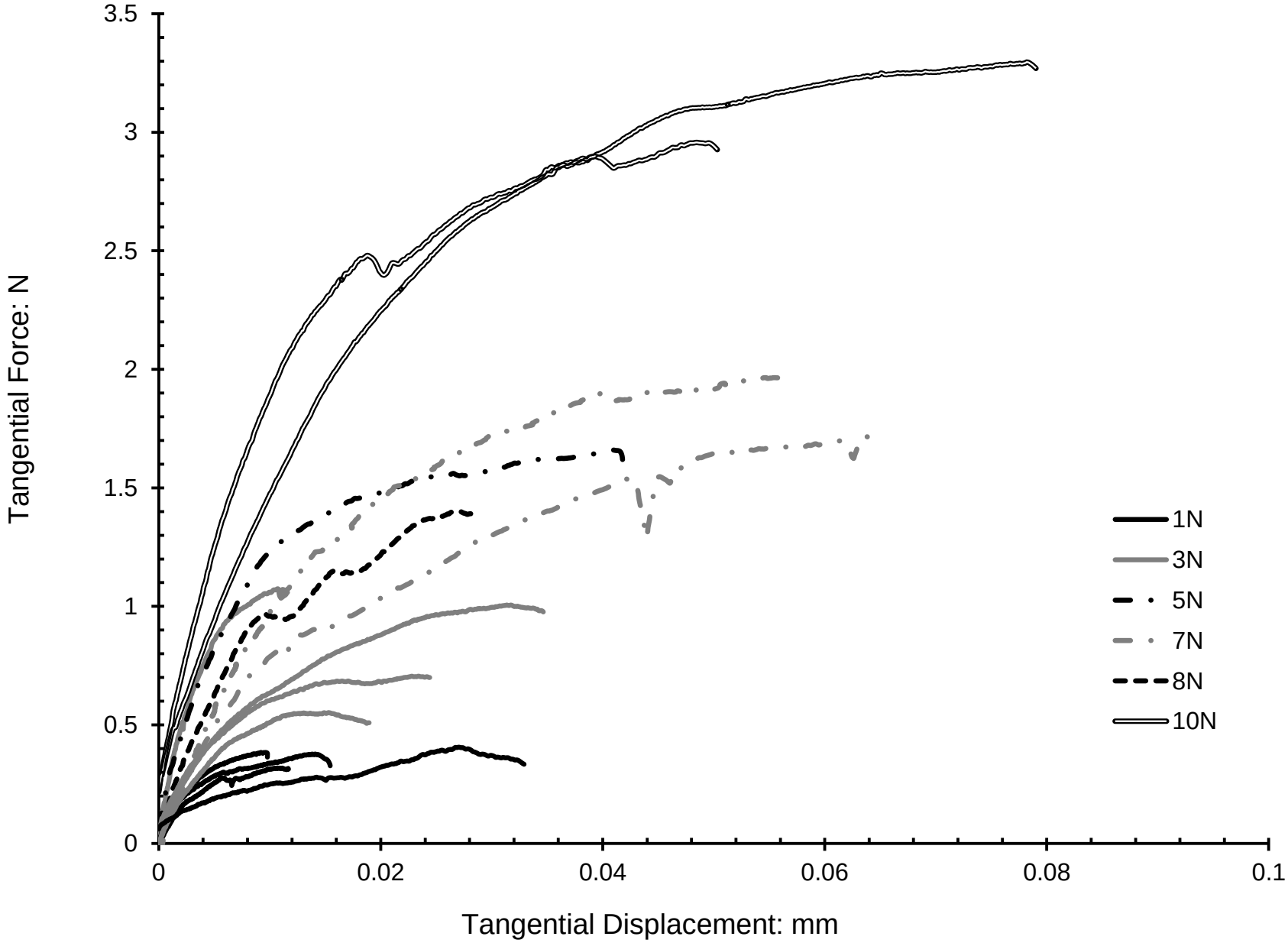

Figure 6

Click here to download Figure Figure 6.xlsx

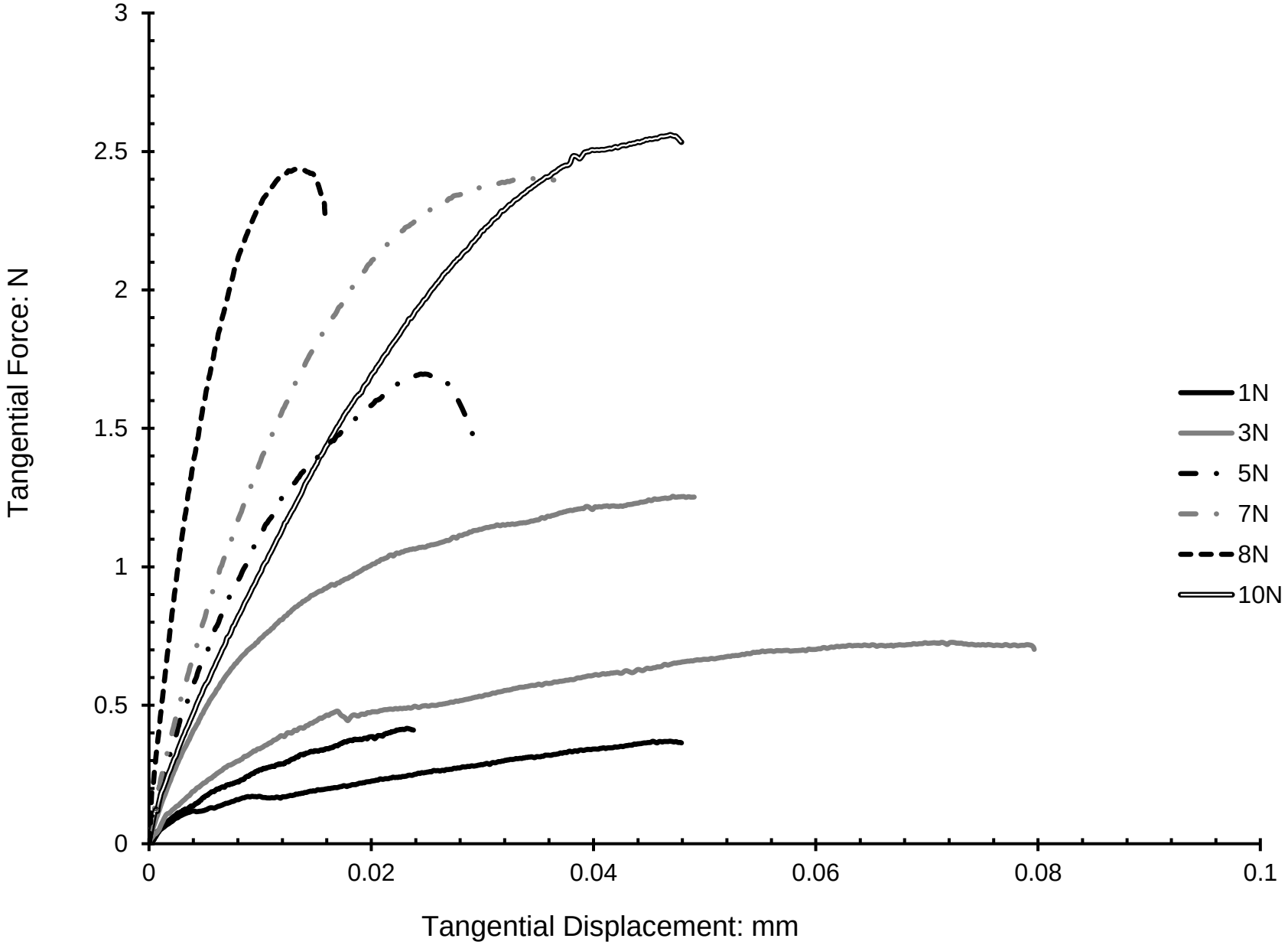

Figure 7

Click here to download Figure Figure 7.xlsx

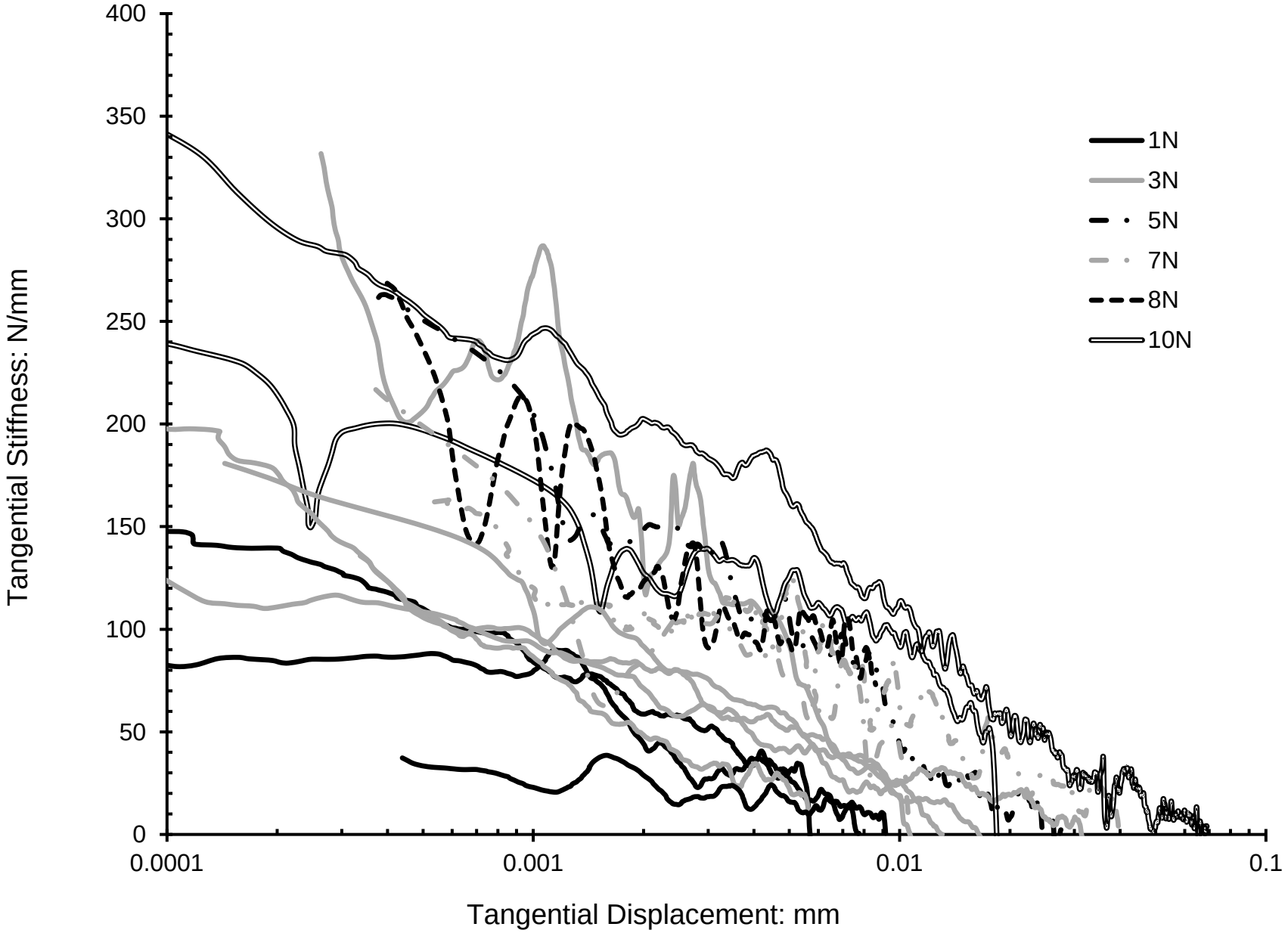

Figure 8

Click here to download Figure Figure 8.xlsx

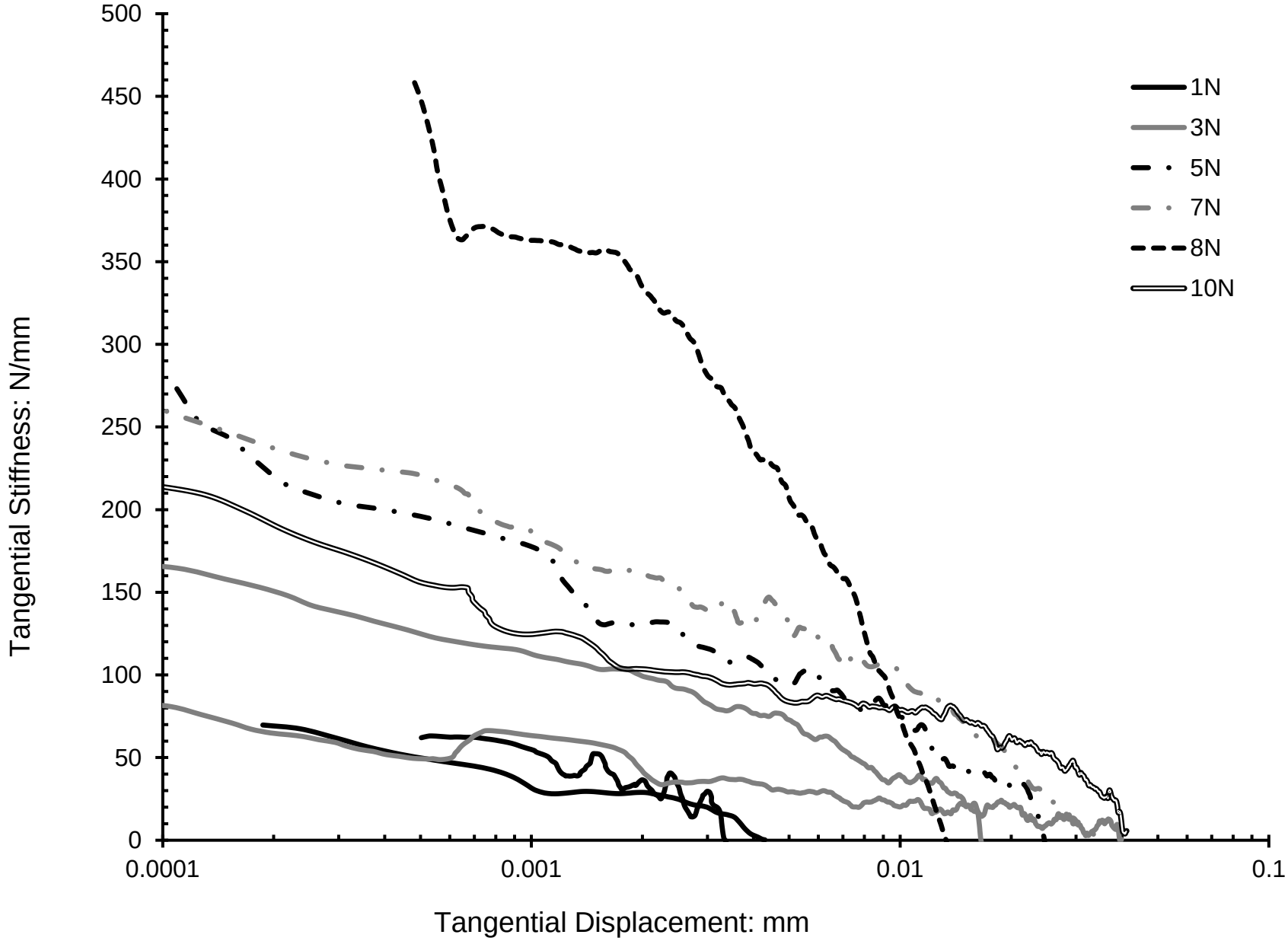

Figure 9

Click here to download Figure Figure 9.xlsx

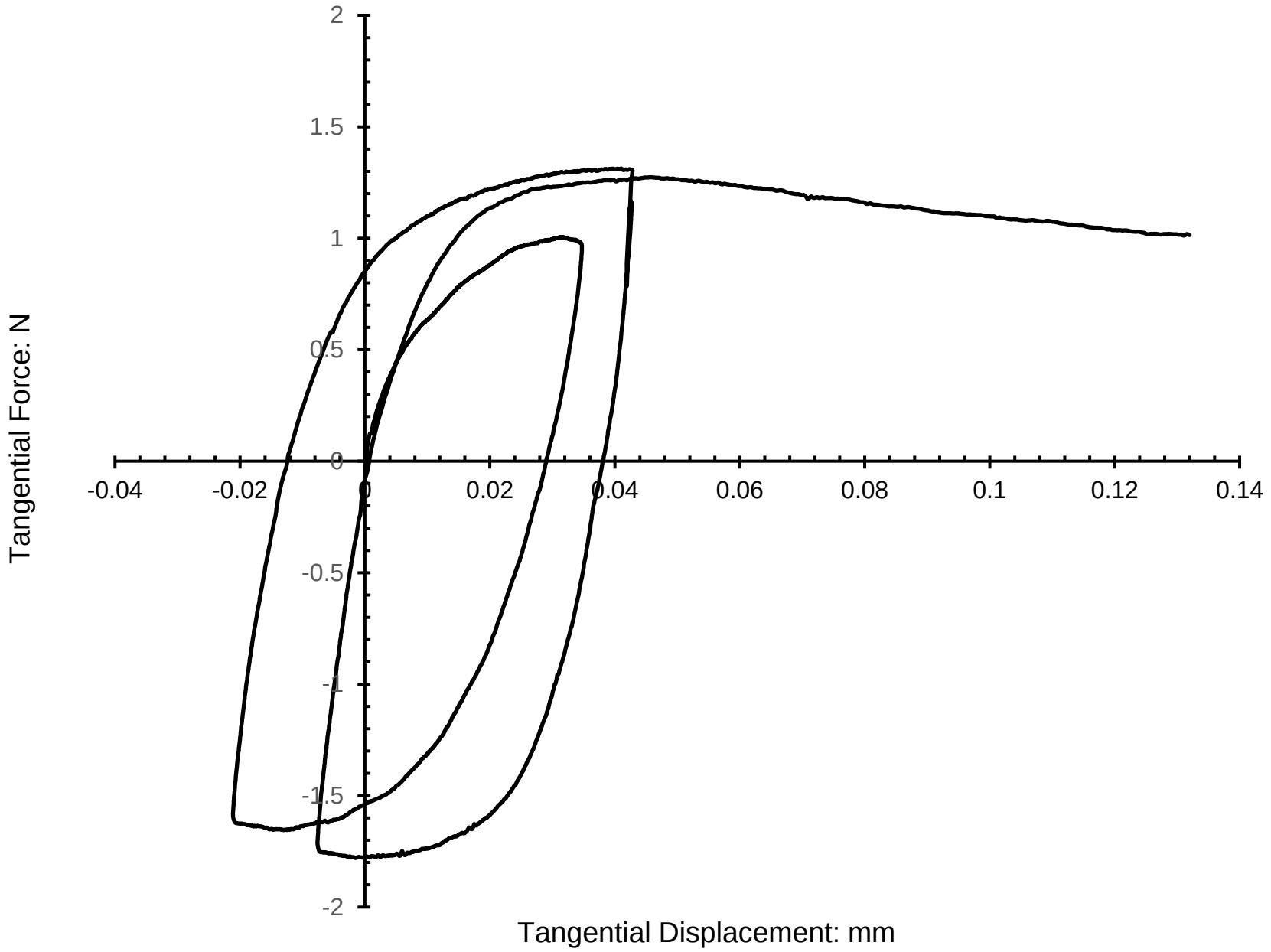

Figure 10

Click here to download Figure Figure 10.xlsx

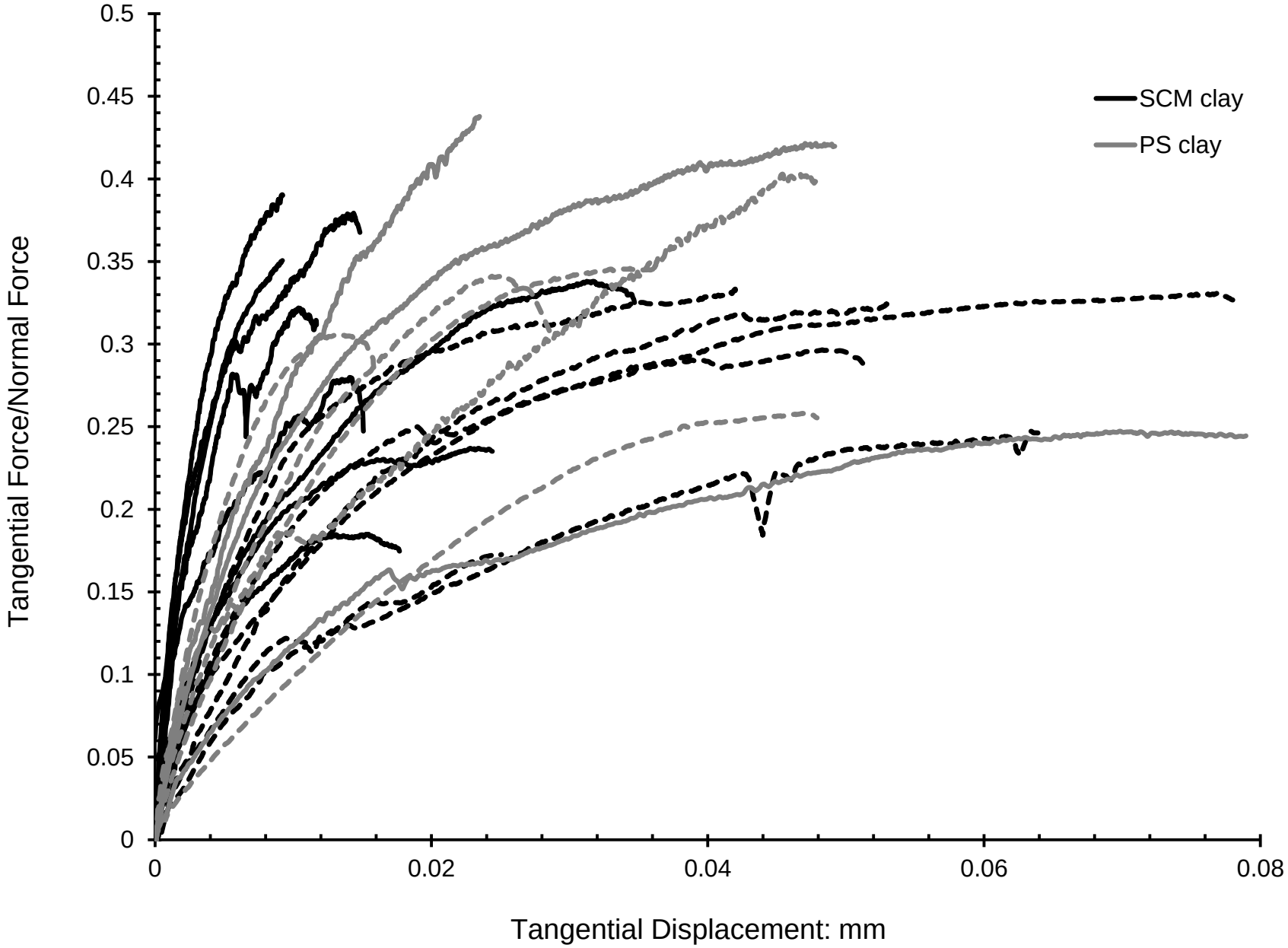

Figure 11

Click here to download Figure Figure 11.xlsx

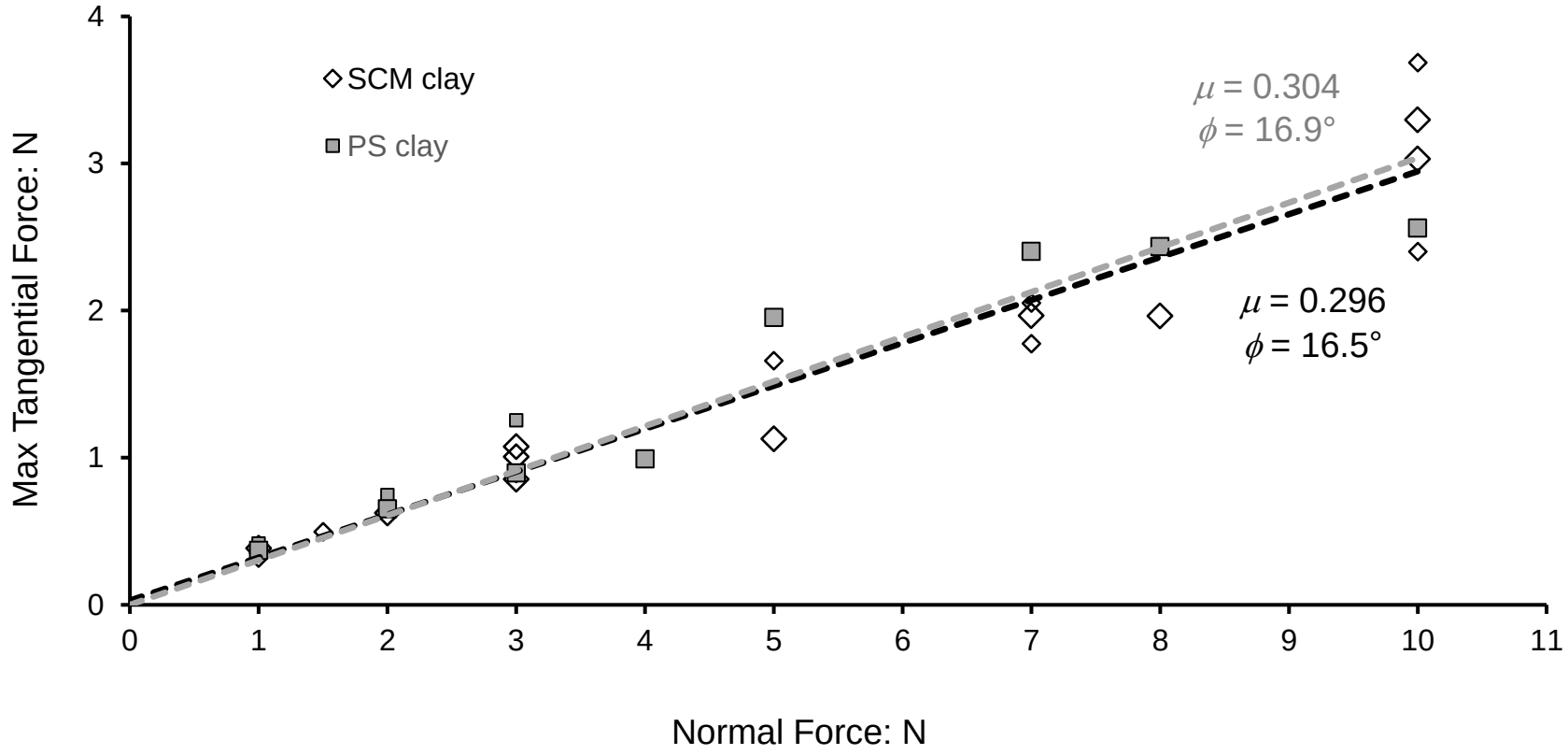

Figure 12

Click here to download Figure Figure 12.xlsx

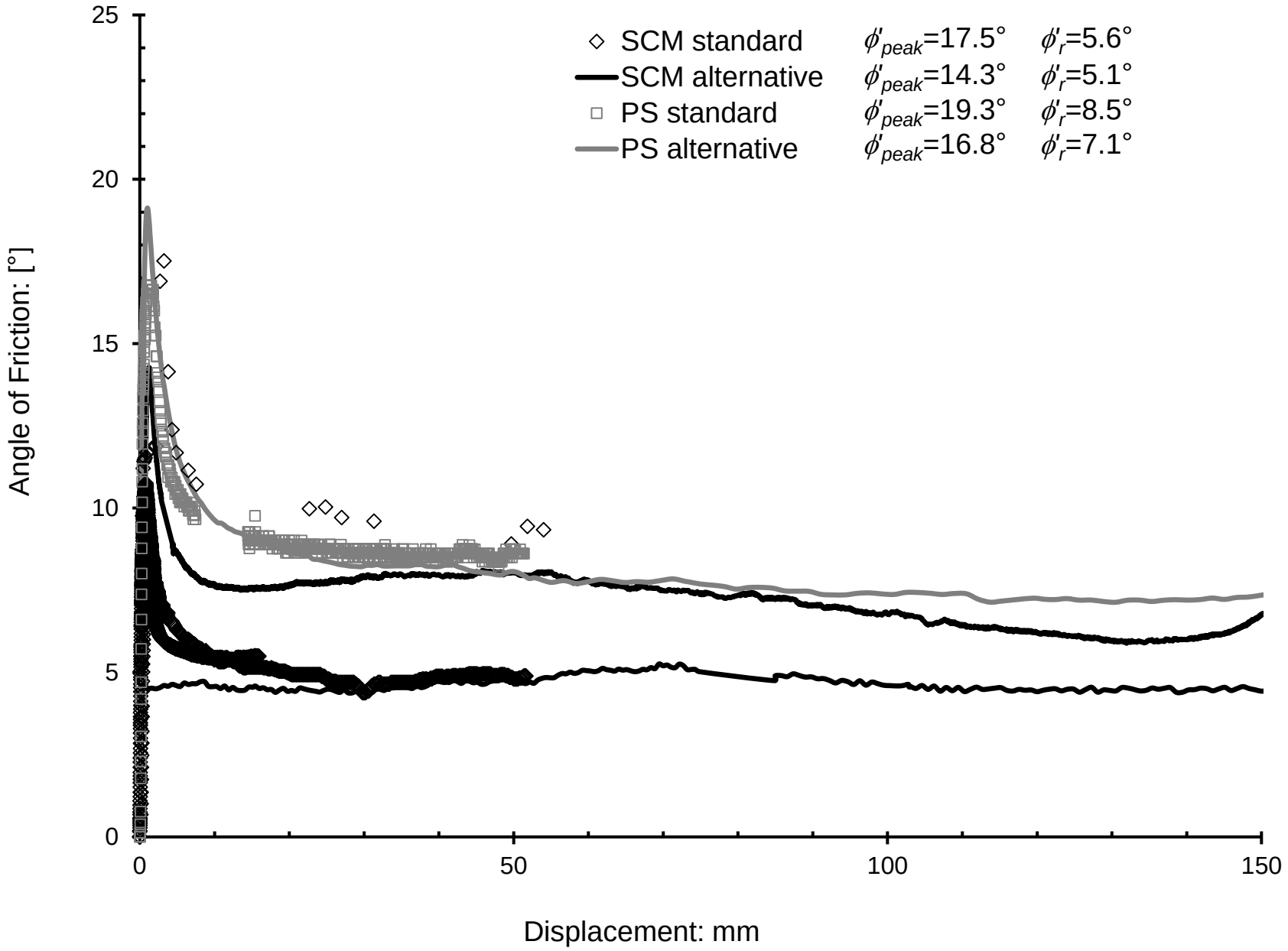

Table 1. Summary of the friction angles found here and in the literature for SCM and PS scaly clays.

Soil type	Testing device	Friction angle
SCM clay	Triaxial apparatus†	ϕ'_{peak}=25°, $\phi'_{post\text{-}peak}$=12-20° ϕ^*_{cs}=18°
	Ring shear apparatus	ϕ'_{peak}=17.5°, ϕ'_{r}=5.6°
	Inter-particle loading apparatus	ϕ =16.5°
PS clay	Triaxial apparatus§	ϕ'_{peak}=21-25°, $\phi'_{post\text{-}peak}$=13-20° ϕ^*_{cs}=18°
	Ring shear apparatus	ϕ'_{peak}=19.3°, ϕ'_{r}=8.5°
	Inter-particle loading apparatus	ϕ =16.9°

†: data from Vitone and Cotecchia (2011)

§: data from Cotecchia et al. (2014)